International Journal of
Molecular Sciences

MDPI

Article

Using Genomic Variation to Distinguish Ovarian High-Grade Serous Carcinoma from Benign Fallopian Tubes

Jesus Gonzalez-Bosquet [1,*], Nicholas D. Cardillo [2], Henry D. Reyes [3], Brian J. Smith [4], Kimberly K. Leslie [5], David P. Bender [1], Michael J. Goodheart [1] and Eric J. Devor [1]

[1] Department of Obstetrics and Gynecology, University of Iowa, 200 Hawkins Dr., Iowa City, IA 52242, USA
[2] Hanjani Institute of Gynecologic Oncology, Thomas Jefferson University, Philadelphia, PA 19107, USA
[3] Department of Obstetrics and Gynecology, University of Buffalo, Buffalo, NY 14203, USA
[4] Department of Biostatistics, University of Iowa, 145 N Riverside Dr., Iowa City, IA 52242, USA
[5] Division of Molecular Medicine, Departments of Internal Medicine and Obstetrics and Gynecology, The University of New Mexico Comprehensive Cancer Center, 915 Camino de Salud, CRF 117, Albuquerque, NM 87131, USA
* Correspondence: jesus-gonzalezbosquet@uiowa.edu; Tel.: +1-(319)-356-2160; Fax: +1-(319)-353-8363

A

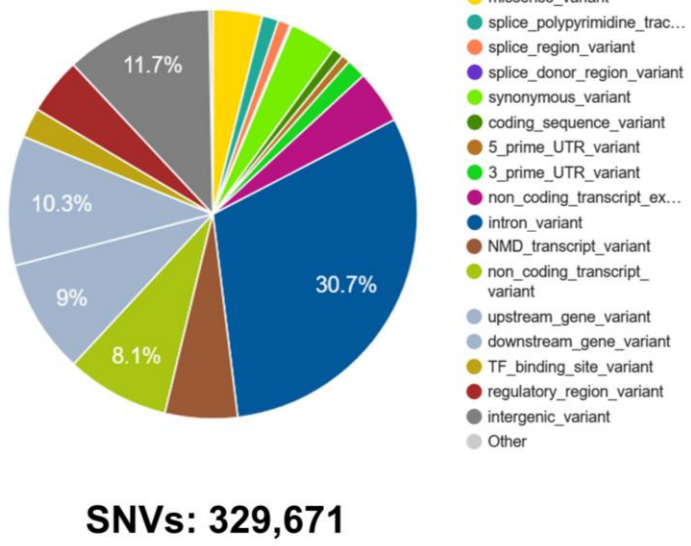

B

Consequence type	Count
splice_acceptor_variant	184
splice_donor_variant	197
stop_gained	266
splice_donor_5th_base_variant	179
frameshift_variant	188
stop_lost	49
start_lost	48
inframe_insertion	37
inframe_deletion	253
missense_variant	20,360
protein_altering_variant	2
splice_polypyrimidine_tract_variant	4,242
splice_region_variant	1,283
incomplete_terminal_codon_variant	2
splice_donor_region_variant	585
synonymous_variant	17,083
stop_retained_variant	16
coding_sequence_variant	8,324
mature_miRNA_variant	6
5_prime_UTR_variant	3,424
3_prime_UTR_variant	4,439
non_coding_transcript_exon_variant	20,458
intron_variant	63,304
non_coding_transcript_variant	1
upstream_gene_variant	9,128
downstream_gene_variant	3,663
TF_binding_site_variant	6,641
regulatory_region_variant	17,139
intergenic_variant	148,170

Supplementary Figure S1. Analysis of all SNVs from one of the HGSC samples analyzed with VEP (Variant Effect Predictor) which predicts the functional effects of genomic variants. **A.** Distribution of all predicted functional consequences of the SNVs found in pie format. **B.** Same variants in table format to report all SNVs numbers (some SNVs may be in several categories).

A

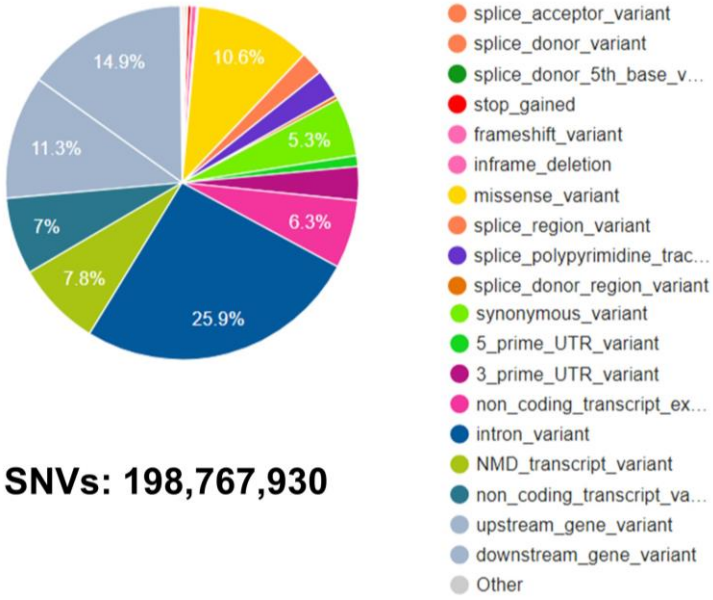

SNVs: 198,767,930

B

Consequence Type	Count
transcript_ablation	23
splice_acceptor_variant	349,294
splice_donor_variant	374,368
splice_donor_5th_base_variant	298,585
stop_gained	650,535
frameshift_variant	970,774
stop_lost	30,535
start_lost	69,805
inframe_insertion	133,479
inframe_deletion	323,810
protein_altering_variant	10,506
missense_variant	21,127,593
splice_region_variant	4,234,450
splice_polypyrimidine_tract_variant	5,112,132
splice_donor_region_variant	731,012
incomplete_terminal_codon_variant	5,383
synonymous_variant	10,632,989
stop_retained_variant	14,845
start_retained_variant	1,033
coding_sequence_variant	43,894
mature_miRNA_variant	12,216
5_prime_UTR_variant	2,000,244
3_prime_UTR_variant	6,099,521
non_coding_transcript_exon_variant	12,445,778
intron_variant	51,485,930
NMD_transcript_variant	15,468,345
non_coding_transcript_variant	13,963,897
upstream_gene_variant	22,481,881
downstream_gene_variant	29,678,694
intergenic_variant	16,379

Supplementary Figure S2. Analysis of all GNOMAD WES population SNVs with VEP. **A.** Distribution of all predicted functional consequences of SNVs in pie format. **B.** Same data in table format to report all SNVs numbers by their downstream effects.

Supplementary Table S1: Pathway analysis of genes including 16,636 variants. Pathway enrichment analysis were performed with *clusterProfiler*, R package, which interrogates *KEGG* database. Represented are significant pathways with their ID, description, p-value and adjusted p-value for multiple comparisons.

ID	Description	p.adjust	geneID
hsa04974	Protein digestion and absorption	<0.001	CELA3A/COL11A1/COL4A3/COL6A6/SLC36A1/ATP1A4/SLC3A1/COL4A4/COL25A1/COL23A1/COL11A2/COL12A1/PRSS2/COL5A1/COL17A1/COL4A1/COL4A2/COL6A1/CELA3B/COL9A2/COL24A1/SLC8A1/COL5A2/COL6A3/SLC36A2/COL21A1/SLC16A10/COL28A1/COL26A1/COL14A1/COL22A1/COL27A1/ATP1B2/COL1A1/COL6A2/COL4A6/PRSS1/PRCP/CPB2/COL5A3/COL20A1/COL18A1/ATP1A2/SLC9A3/SLC6A19/SLC36A3/MEP1A/COL19A1/COL13A1/CTRB1/KCNN4/COL2A1/SLC7A7/SLC15A1/ATP1A3/COL9A1/ACE2/CELA2A/SLC1A5
hsa04070	Phosphatidylinositol signaling system	<0.001	PIK3C2B/INPP4B/DGKB/PI4KA/ITPR1/CDS1/SYNJ2/MTMR7/PLCE1/MTMR6/PLCB2/PLCG2/DGKE/PIK3R3/CALM2/PIKFYVE/PIK3R1/DGKI/PIP5K1B/PIK3C2A/PIK3C2G/PIP4K2C/DGKH/SYNJ1/MTM1/MTMR1/PLCD1/PIK3CB/DGKG/CALML4/PRKCA/PI4K2B/MTMR2/INPP5B/PIP5K1A/INPP4A/DGKD/ITPR3/IP6K3/ITPR2/ITPK1/ITPKA/PRKCB/PIK3C3/PIP5K1C/CDS2/MTMR3/CALML5/CALM1/PIK3R2/IMPA2/IP6K1/CALM3/PLCB1/IP6K2/PLCZ1
hsa04512	ECM-receptor interaction	<0.001	COL4A3/COL6A6/FRAS1/LAMA5/ITGB6/ITGAV/FN1/COL4A4/DMP1/SV2C/LAMA2/THBS2/FREM1/COL4A1/COL4A2/ITGA11/LAMA1/LAMA3/COL6A1/COL9A2/TNR/COL6A3/ITGA2/THBS4/CD36/RELN/LAMC3/VWF/COL1A1/COL6A2/COL4A6/HSPG2/LAMC1/LAMA4/LAMB1/ITGB1/AGRN/TNN/LAMB3/SDC1/ITGB5/ITGA1/ITGB8/ITGA8/ITGB3/ITGB4/SDC4/NPNT/COL2A1/ITGA2B/COL9A1
hsa04912	GnRH signaling pathway	<0.001	PRKACB/PLA2G4A/CACNA1C/SOS2/GRB2/ITPR1/MAPK10/ADCY2/CAMK2B/PTK2B/ADCY4/PLCB2/ADCY9/CALM2/CACNA1D/MAP3K1/MAPK9/PLA2G4D/PLA2G4F/GNAS/CACNA1S/SOS1/ADCY5/ADCY1/CAMK2G/CALML4/PRKCA/NRAS/MAP3K2/RAF1/CAMK2A/ITPR3/MAPK14/ITPR2/PLA2G4E/PRKCB/MMP2/CALML5/KRAS/MAP3K4/MAPK12/PRKCD/CALM1/FSHB/MAPK1/GNA11/GNAQ/CALM3/PLCB1/ADCY8/PLD2/PLA2G4C
hsa05412	Arrhythmogenic right ventricular cardiomyopathy	<0.001	CACNA1C/RYR2/ITGB6/ITGAV/LAMA2/CACNA2D1/CACNB2/PKP2/ITGA11/LAMA1/ACTN2/SLC8A1/TCF7L1/CACNA1D/CACNA2D3/ITGA2/CTNNA3/CDH2/DSC2/DMD/CACNA1S/LEF1/CTNNA1/DSP/ITGB1/SGCA/CACNG6/CACNG1/CTNNA2/ITGB5/ITGA1/ITGB8/ITGA8/CACNA2D4/JUP/ITGB3/ITGB4/DSG2/ATP2A3/ATP2A1/ITGA2B/CACNG2/CACNB4/DES
hsa04925	Aldosterone synthesis and secretion	<0.001	PRKACB/CACNA1C/ATP1A4/ATP2B4/ITPR1/ADCY2/CAMK2B/ADCY4/PRKD1/PLCB2/CACNA1H/ADCY9/CACNA1G/CACNA1I/CALM2/CACNA1D/ATP1B2/GNAS/CACNA1S/PRKD3/PRKCE/ADCY5/CAMK4/CREB5/ADCY1/CAMK1D/CAMK2G/CALML4/PRKCA/ATP1A2/ATP2B2/CAMK2A/ITPR3/DAGLB/CREB3L2/CREB3L1/ITPR2/PRKCB/CALML5/DAGLA/CALM1/CREB3L3/ATP2B1/ATP1A3/CYP11B2/CYP11A1/GNA11/GNAQ/LDLR/CALM3/PRKD2/PLCB1/ADCY8
hsa04510	Focal adhesion	<0.001	COL4A3/MYLK/COL6A6/RAP1B/SOS2/GRB2/SHC2/PAK4/LAMA5/VAV3/ROCK2/ITGB6/ITGAV/FN1/COL4A4/MAPK10/FLT4/LAMA2/THBS2/RAC1/TLN1/VAV2/COL4A1/COL4A2/ITGA11/LAMA1/LAMA3/COL6A1/COL9A2/PIK3R3/TNR/COL6A3/FLNB/PDGFRA/KDR/ITGA2/PIK3R1/THBS4/MAPK9/RELN/PIP5K1B/LAMC3/DOCK1/PARVA/VWF/PAK6/COL1A1/MYL12A/ACTN4/COL6A2/COL4A6/LAMC1/PPP1R12B/SOS1/PIK3CB/PAK2/LAMA4/LAMB1/CAV1/ITGB1/PDGFD/PRKCA/CRKL/PIP5K1A/TNN/LAMB3/AKT3/RAF1/ITGB5/ITGA1/MYLK4/ITGB8/ITGA8/PAK1/PRKCB/ITGB3/ITGB4/PIP5K1C/FLT1/RASGRF1/ARHGAP35/CCND3/COL2A1/ITGA2B/VAV1/PIK3R2/MYLK3/ERBB2/MAPK1/CRK/RHOA/COL9A1/FYN/VASP
hsa04750	Inflammatory mediator regulation of TRP channels	0.001	PRKACB/PLA2G4A/ALOX12/ITPR1/IL1RAP/MAPK10/ADCY2/CAMK2B/TRPA1/ADCY4/PLCB2/ADCY9/PLCG2/TRPV3/PIK3R3/CALM2/IL1B/PIK3R1/MAPK9/PRKCH/PLA2G4D/PLA2G4F/TRPV1/GNAS/NTRK1/PRKCE/ADCY5/PIK3CB/ADCY1/CAMK2G/CALML4/PRKCA/PLA2G6/KNG1/CAMK2A/ITPR3/MAPK14/ITPR2/PLA2G4E/PRKCB/CALML5/MAPK12/PRKCD/CALM1/PIK3R2/ASIC1/GNAQ/CALM3/PLCB1/ADCY8/BDKRB2/PLA2G4C
hsa04921	Oxytocin signaling pathway	0.001	PRKACB/PLA2G4A/MYLK/CACNA1C/NFATC1/PRKAA2/RYR2/ROCK2/ITPR1/ADCY2/MEF2C/CAMK2B/CACNA2D1/CACNB2/ADCY4/RYR3/PLCB2/ADCY9/CALM2/CACNA1D/CACNA2D3/GUCY1A1/PRKAA1/NFATC4/PLA2G4D/PLA2G4F/MAP2K5/PIK3R5/RYR1/GNAS/TRPM2/CACNA1S/PPP1R12B/ADCY5/CAMK4/ADCY1/GNAI1/PRKAG2/CAMK1D/CAMK2G/CALML4/PRKCA/CACNG6/CACNG1/NRAS/RAF1/CAMK2A/MYLK4/ITPR3/PIK3CG/CACNA2D4/ITPR2/CAMKK2/PLA2G4E/PRKCB/GNAO1/NFATC2/CDKN1A/CALML5/KRAS/KCNJ18/CACNG2/CACNB4/CALM1/MYLK3/MAPK1/RHOA/GNAQ/PIK3R6/CALM3/PLCB1/OXTR/ADCY8/PLA2G4C
hsa04072	Phospholipase D signaling pathway	0.001	PLA2G4A/DGKB/SOS2/TSC2/GRB2/SHC2/ADCY2/GRM1/PTK2B/ADCY4/ARF6/PLCB2/ADCY9/PLCG2/DGKE/CYTH1/INSR/LPAR4/MTOR/PIK3R3/GRM7/PDGFRA/GAB1/PIK3R1/GNA12/DGKI/AGPAT5/PIP5K1B/F2/AVPR1A/DGKH/PLA2G4D/PLA2G4F/PIK3R5/GNAS/SOS1/ADCY5/PIK3CB/DGKG/ADCY1/PDGFD/PRKCA/AVP/RHEB/GRM8/NRAS/PIP5K1A/AKT3/RALB/DGKD/RAF1/PIK3CG/RALGDS/PLA2G4E/PIP5K1C/KRAS/TSC1/PIK3R2/GRM4/MAPK1/FCER1A/RAPGEF4/RHOA/FYN/PIK3R6/PLPP2/PLCB1/ADCY8/INS/PLD2/PLA2G4C

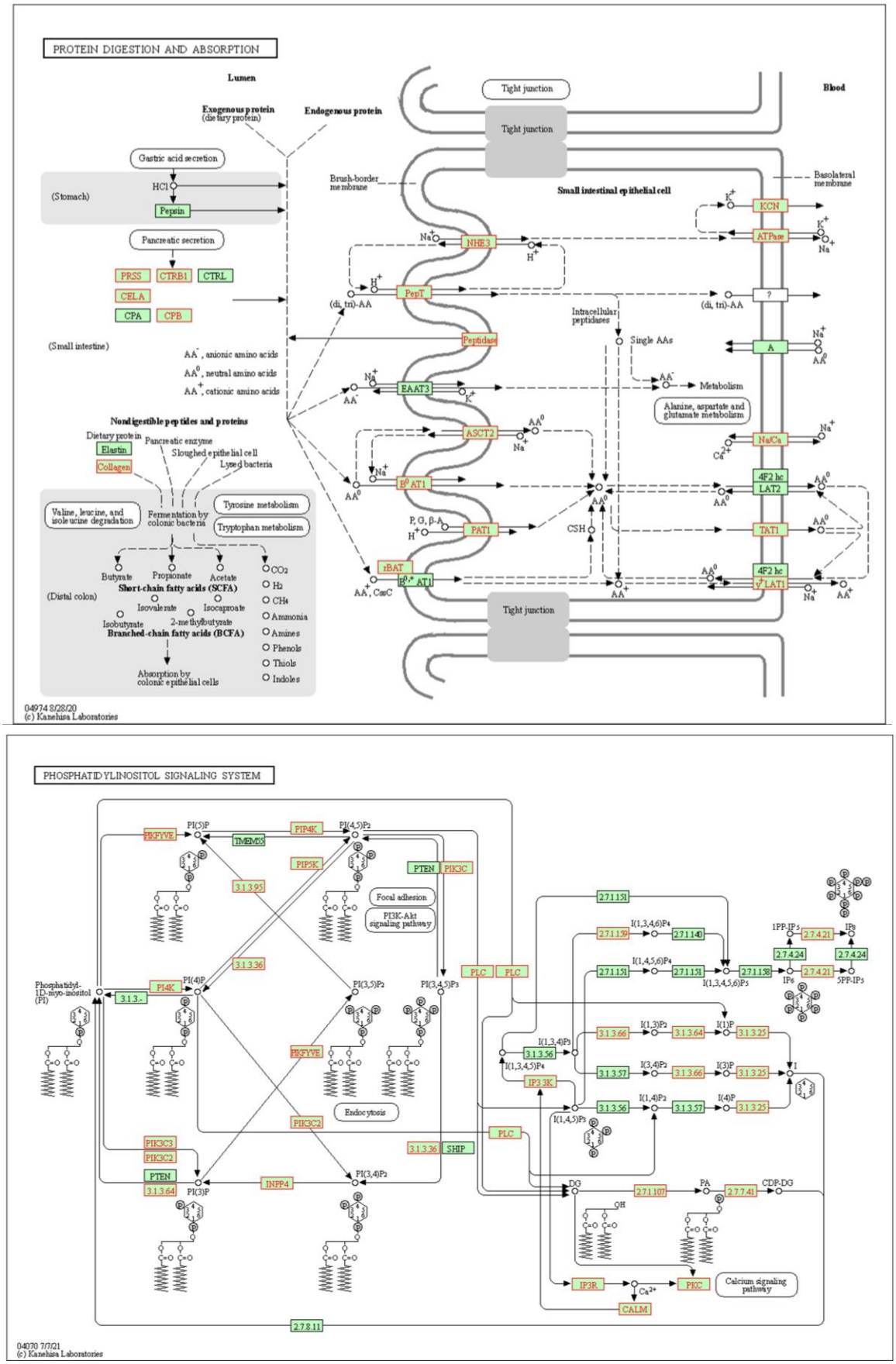

Supplementary Figure S3. Significant pathways 'Protein digestion and absorption' and 'Phosphatidylinositol signaling system' from KEGG database (adjusted p-value for multiple comparisons: <0.001)(printed with copyright permission of KEGG).

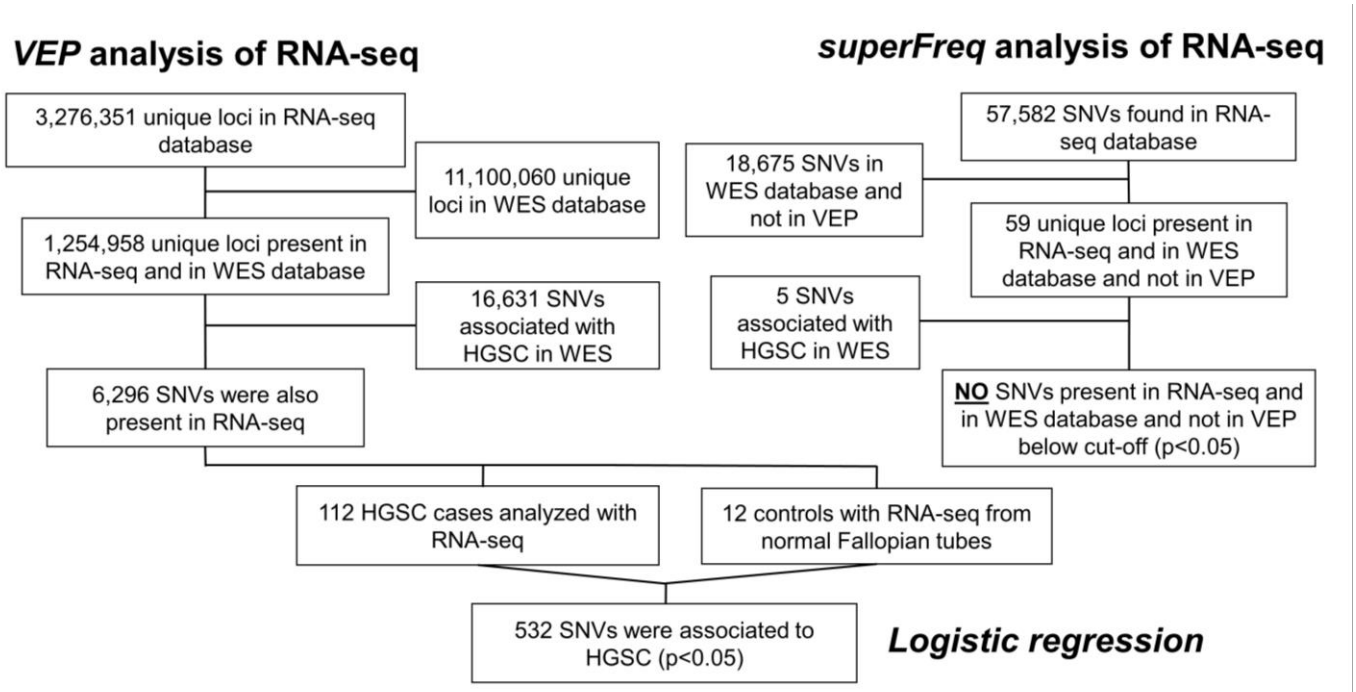

Supplementary Figure S4. Validation analysis in RNA-seq data**.**

Variation analysis with VEP in RNA-seq data. Of the initial more than 3 million SNVs found in all HGSC samples, over 1.2 million were also present in WES VEP analysis. Out of the initial 16,631 selected SNVs, associated with HGSC in the WES VEP analysis, 6,296 SNVs were also present in RNA-seq VEP analysis (Fig. 1). Unrelated controls consisted in 12 RNA-seq samples from the distal part of the Fallopian tube (fimbria) from patients with no disease and no family history of ovarian cancer. It resulted in 532 SNVs associated with HGSC (p-value < 0.05).

Variation analysis with superFreq in RNA-seq data. Of the initial more than 57 thousand SNVs found in all HGSC samples after quality filters, 59 were also present in WES superFreq analysis (Fig. 1). None of these SNVs passed the cut-off after the initial univariate logistic analysis.

Supplementary Table S2: Pathway analysis of genes including 532 variants. Pathway enrichment analysis were performed with *clusterProfiler*, R package, which interrogates *KEGG* database. Represented are significant pathways with their ID, description, p-value and adjusted p-value for multiple comparisons.

ID	Description	pvalue	p.adjust	Symbol
hsa04068	FoxO signaling pathway	<0.001	0.013	INSR/TGFB3/HOMER2/FBXO32/PIK3R1/MDM2/GRB2/RAF1/FOXO3/ATM/MAPK10/USP7
hsa04912	GnRH signaling pathway	<0.001	0.013	CALM2/CALML4/GRB2/ADCY8/RAF1/MAP3K1/PLCB1/PLA2G4A/MAPK10/ADCY4
hsa04218	Cellular senescence	<0.001	0.013	HLA-F/CALM2/TGFB3/CDK1/PIK3R1/MRE11/MDM2/CALML4/RAF1/FOXO3/NFATC2/ATM/HLA-A
hsa04072	Phospholipase D signaling pathway	<0.001	0.023	INSR/RALGDS/PIK3R1/FYN/GRB2/ADCY8/RAF1/PLCB1/CYTH1/PLPP2/PLA2G4A/ADCY4
hsa04015	Rap1 signaling pathway	0.001	0.045	INSR/CALM2/MAGI1/RALGDS/PIK3R1/CALML4/FARP2/ADCY8/RAF1/DOCK4/PLCB1/ANGPT2/FLT4/ADCY4
hsa04660	T cell receptor signaling pathway	0.001	0.049	PIK3R1/FYN/GRB2/RAF1/NFATC2/MAPK10/TEC/CD4/RASGRP1
hsa05210	Colorectal cancer	0.001	0.049	BAK1/RALGDS/TGFB3/PIK3R1/GRB2/RAF1/MAPK10/MSH3
hsa05163	Human cytomegalovirus infection	0.002	0.049	HLA-F/CALM2/BAK1/PIK3R1/MDM2/CALML4/GRB2/ADCY8/RAF1/NFATC2/PLCB1/CASP8/ADCY4/HLA-A
hsa05203	Viral carcinogenesis	0.002	0.049	HLA-F/BAK1/PSMC1/CDK1/PIK3R1/MDM2/GSN/SND1/GRB2/CASP8/USP7/KAT2B/HLA-A
hsa05205	Proteoglycans in cancer	0.002	0.049	ANK3/EIF4B/ESR1/IQGAP1/WNT5B/ERBB4/PIK3R1/MDM2/PPP1R12B/GRB2/RAF1/EZR/GPC1
hsa01524	Platinum drug resistance	0.002	0.049	BAK1/PIK3R1/MDM2/REV3L/ATM/CASP8/MSH3
hsa04915	Estrogen signaling pathway	0.002	0.049	CALM2/ESR1/PIK3R1/CALML4/GRB2/ADCY8/RAF1/FKBP5/PLCB1/ADCY4
hsa05170	Human immunodeficiency virus 1 infection	0.003	0.049	HLA-F/CALM2/BAK1/CDK1/PIK3R1/CALML4/RAF1/NFATC2/ATM/CASP8/MAPK10/CD4/HLA-A
hsa05214	Glioma	0.003	0.049	CALM2/BAK1/PIK3R1/MDM2/CALML4/GRB2/RAF1
hsa04935	Growth hormone synthesis, secretion and action	0.003	0.049	PIK3R1/GRB2/ADCY8/RAF1/MAP3K1/PLCB1/GHR/MAPK10/ADCY4
hsa01522	Endocrine resistance	0.003	0.049	ESR1/PIK3R1/MDM2/GRB2/ADCY8/RAF1/MAPK10/ADCY4
hsa04750	Inflammatory mediator regulation of TRP channels	0.003	0.049	CALM2/PIK3R1/CALML4/ADCY8/PLCB1/PLA2G4A/MAPK10/ADCY4
hsa05231	Choline metabolism in cancer	0.003	0.049	CHPT1/RALGDS/PIK3R1/GRB2/RAF1/PLPP2/PLA2G4A/MAPK10/

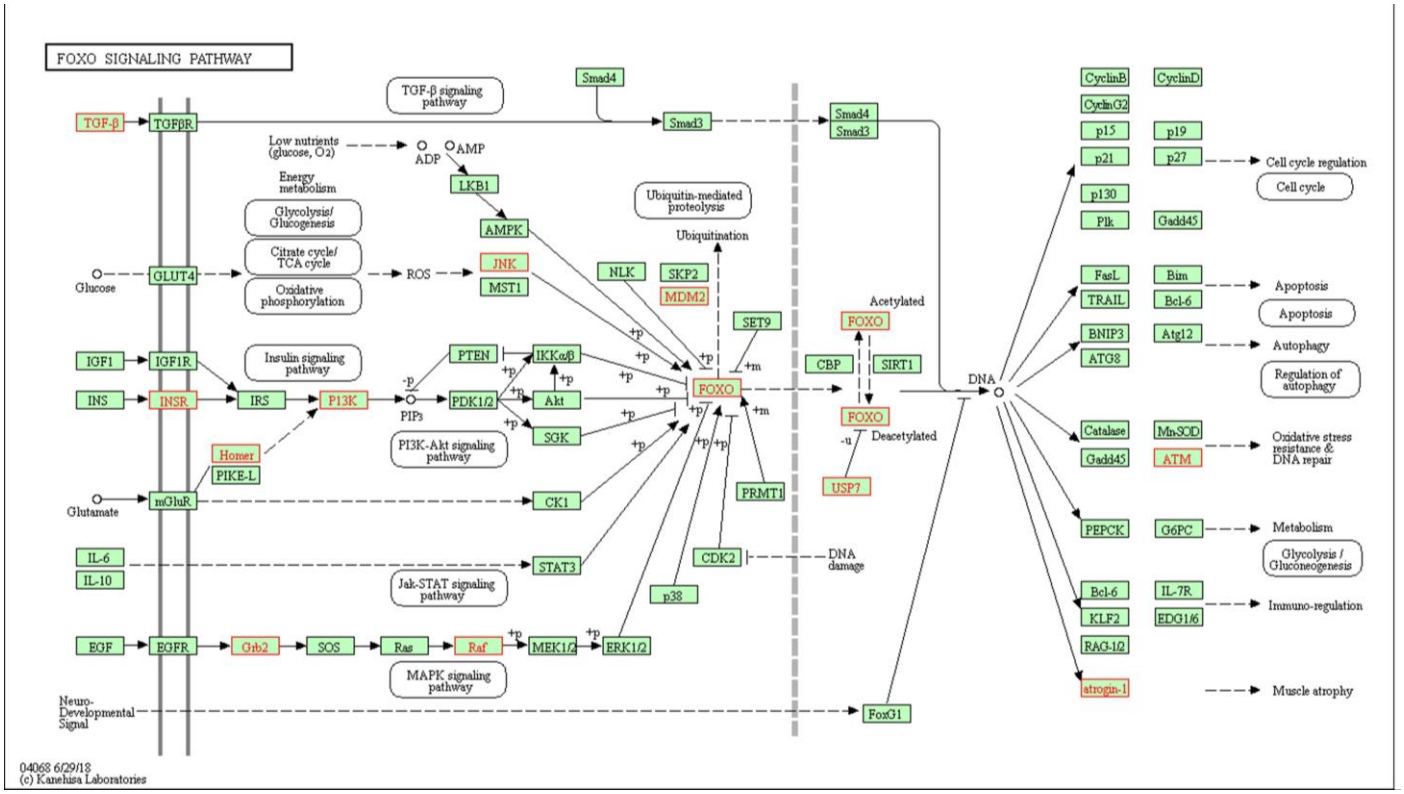

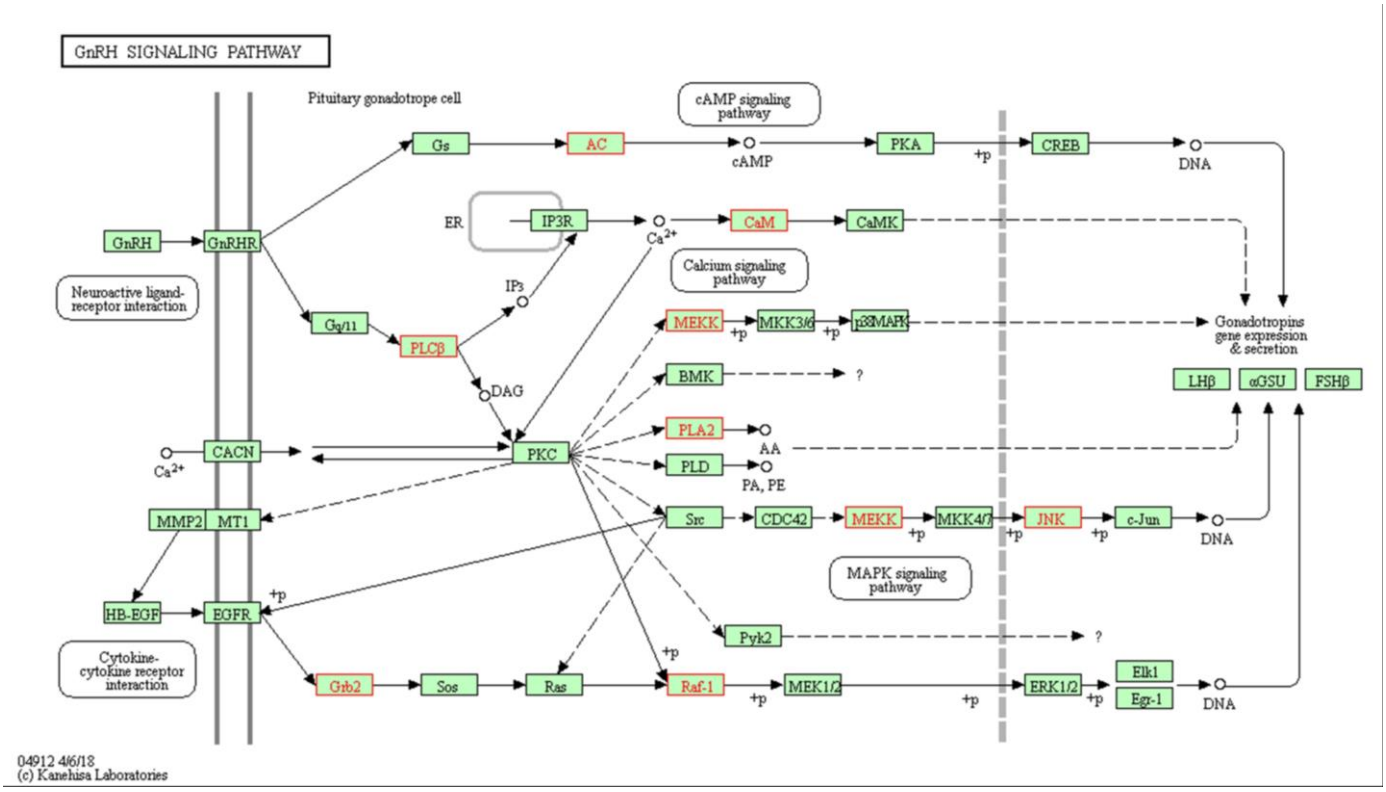

Supplementary Figure S5. Significant pathway 'FoxO signaling pathway' and 'GnRH signaling pathway' from KEGG database (adjusted p-value for multiple comparisons: 0.013)(printed with copyright permission of KEGG).

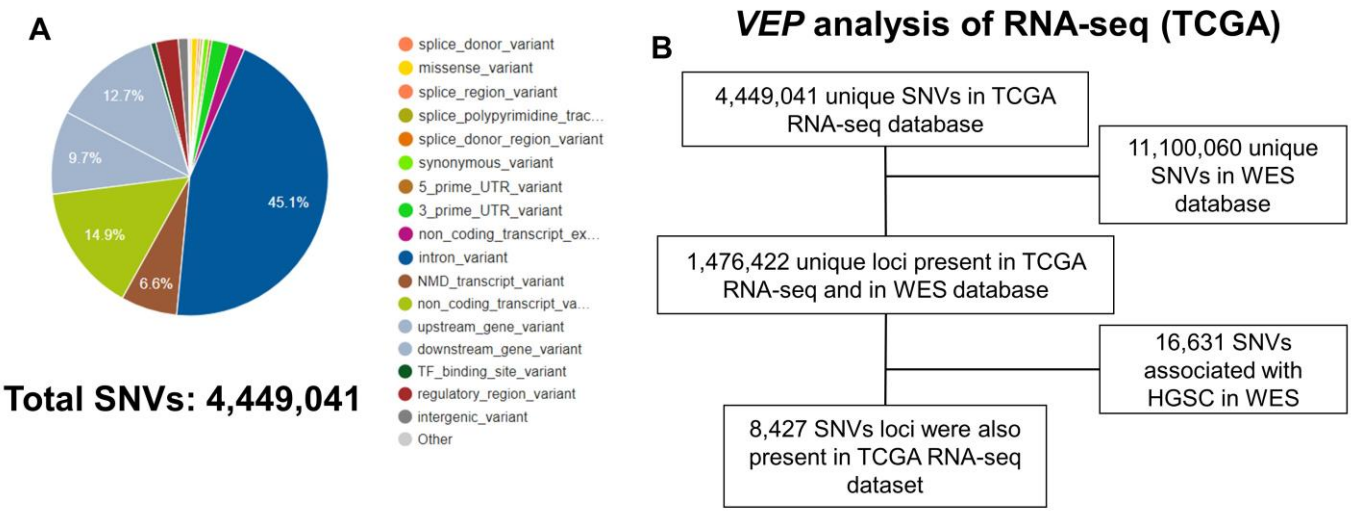

Supplementary Figure S6. Analysis of all SNVs from all TCGA HGSC RNA-seq dataset analyzed with VEP. A. Distribution of all predicted functional consequences of the SNVs found in a pie format. B. Of the initial almost 4.5 million SNVs found in all TCGA HGSC samples, over 1.4 million were also present in WES VEP analysis (and not in the gnomAD database, Fig. 1). Also, out of the initial 16,631 selected SNVs, associated with HGSC in the WES VEP analysis, 8,427 SNVs were also present in TCGA RNA-seq VEP analysis. Unfortunately, there are no normal samples that were sequenced in TCGA to use as controls.

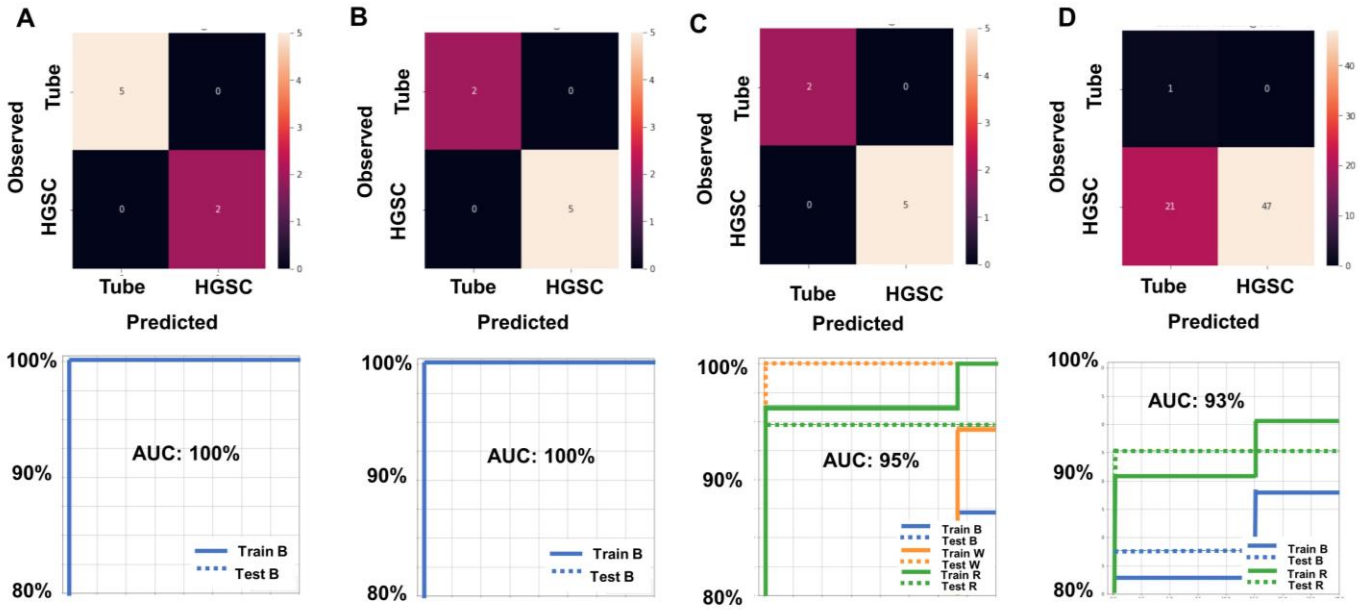

Supplementary Figure S7. Validation of WES DNA SNV prediction model of HGSC performed in RNA-seq samples with machine learning analytical platform.

A. Model with all SNV associated with HGSC (N=16,631). The superior panel shows the confusion matrix representing the observed versus the predicted values. The inferior panel is an ROC graphic: true positives in the x axis, false positives in the y axis, and AUC results. Train B: results of baseline training; Test B: results of baseline testing. **B.** Model resulting from the multivariate analysis with lasso (N=49). Superior and inferior panels are as before. **C.** Model with UI RNA-seq SNVs (N=20). Superior panel is as before. Inferior panel represents the ROC graphic including models accounting for weights of the outcome: 1) Train W: results of weighted model training; Test W: results of weighted model testing; 2) Train R: results of unbalanced (or re-sampling) model training; Test R: results of re-sampling model testing. **D.** Model with TCGA RNA-seq SNVs (N=18). Superior panel is as before. Inferior panel represents the ROC graphic including models accounting for weights of the outcome: Train R: results of unbalanced (or re-sampling) model training; Test R: results of re-sampling model testing.

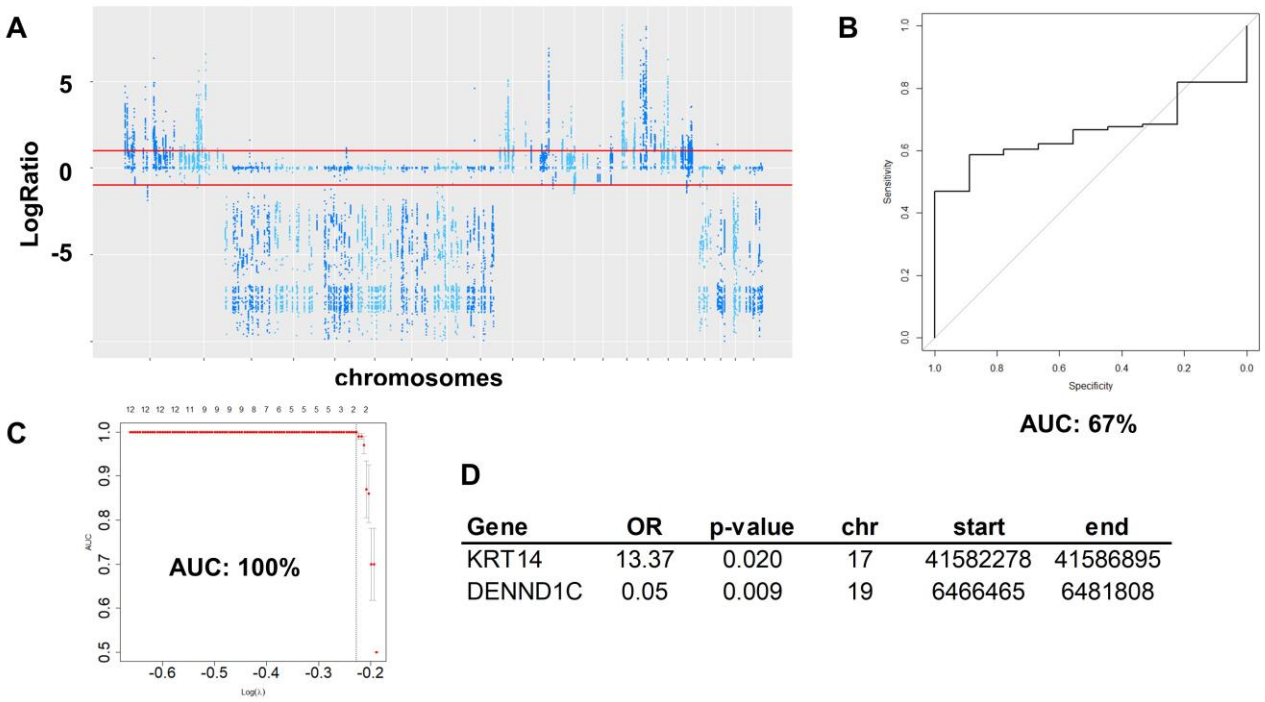

Gene	OR	p-value	chr	start	end
KRT14	13.37	0.020	17	41582278	41586895
DENND1C	0.05	0.009	19	6466465	6481808

Supplementary Figure S8. Validation of WES DNA CNV analysis performed in RNA-seq samples.

A. Manhattan plot representations of all 558 CNV significant in the WES and assessed in the RNA-seq experiment. The red lines represent x2 copies (or more than diploid) and 0.5 copies (or less than heterozygous). There are specific gains and losses in some chromosomes: gains in 1,2,10,11,12,15,16,17, and 19; losses in 3,4,5,6,7,8,9,20,21,22, and X.

B. Validation of the DNA lasso prediction model in RNA-seq data (Fig. 6C), with a fair performance of an AUC of 66%: for a sensitivity of 85% the accuracy was 89% and PPV of 92%.

C. CNV lasso prediction regression analysis performed in RNA-seq samples, not using the lasso model from DNA analysis. ROC curve of this prediction model with 2 genes with CNV: AUC of 100%, (95% CI:100,100). These two CNV, CNTN4-AS1 and ENST00000565823 are protective for HGSC.

D. Logistic regression analysis including the significant 558 CNV in the WES analysis. This analysis was done independently of the WES DNA model. One gene increased the risk, KRT14, the other one decreased, DENND1C.

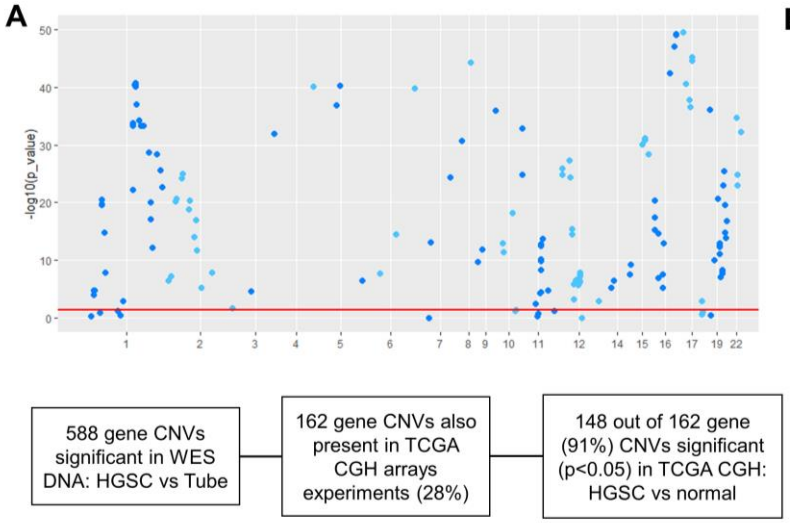

B

Gene	OR	chrom	start	end
CHRFAM7A	0.88	15	28440735	28473156
CPSF2	1.12	14	91658082	91700296
OR2T29	0.83	1	246788468	246789397
PARP15	1.06	3	123817215	123838226
TXNDC9	1.51	2	99301919	99319292
ZNF513	0.60	2	27453606	27457097

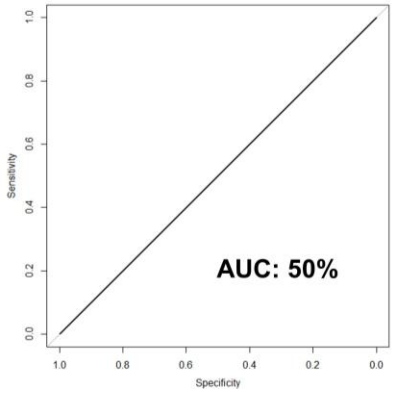

Supplementary Figure S9. Validation of WES DNA CNV analysis performed in TCGA RNA-seq samples.

A. Manhattan plot representations of 162 CNV present in TCGA CGH database, out of the 558 significant CNV in the WES DNA analysis. The red lines represent p-value <0.05. 148 were significant out of 162. **B.** Validation of the DNA lasso prediction model in TCGA RNA-seq data. The WES DNA model was re-done with the 162 genes present in the CGH array TCGA database. The table is the model in WES DNA, that had an AUC of 80% (95% CI 74%, 86%), lower than the full model with 588 genes (87% in Fig. 6). The ROC represents the validation in TCGA dataset with an AUC of 50%, for a sensitivity of 85%, accuracy of 51% and PPV of 51%.

A

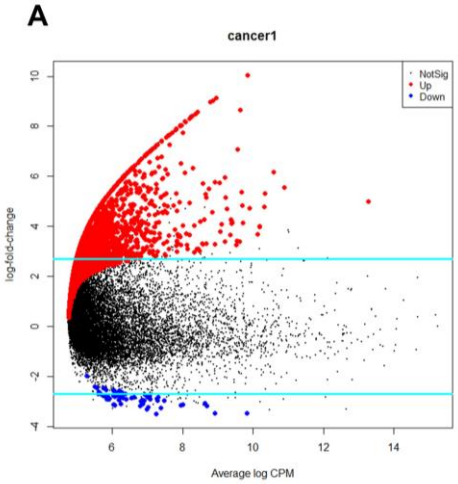

	HGSC
Up	5,928
Not-Sig	26,153
Down	75

B

Structural Variant (SV) type	Number
AS (alternative splicing) -- spliced contig alignment where both junctions are known reference exon boundaries, but spliced reads across these boundaries have not previously been observed.	170
DEL (deletion) -- aligned section of contig that does not contain part of the reference sequence.	126
EE (extended exon) -- contig alignment extends past an exon boundary.	134
FUS (fusion) -- contig involving hard-clipping (one part of the contig aligns to one part of the genome, and the other part aligns elsewhere). Fusions require at least one gene to be involved in all cryptic variants.	480
IGR (intragenic rearrangement) -- hard clipped contig where both parts align within the same gene(s).	135
INS (insertion) -- aligned section of the contig that is not in the reference. This could be a tandem duplication, but is not annotated as such yet	208
NE (novel exon) -- an aligned block that does not cross any existing exons. May be intronic or intergenic.	2164
NEJ (novel exon junction) -- spliced contig where neither junction boundary matches the reference.	1046
PNJ (partial novel junction) -- spliced contig where one junction matches a known boundary (the other side is unknown).	88
RI (retained intron) -- a contig block that spans a whole intron.	436
UN (unknown) -- by default, all soft-clipped contigs are classified as unknown at the moment. These variants need to be better annotated.	4462

Supplementary Figure S10. Univariate analysis of all SV for cases vs controls (package *edgeR*). **A.** Out of 32,156 SVs, 6,003 were below the cut-off in multiple univariate analyses (at $p<0.001$). 75 of them were decreased in HGSC and 5,928 were increased. **B.** The table details the type and number of SV that were significant.

A

SV	chr	start	size	strand	SV type	genes	OR	p-value	95% CI
chr3_147402104_RI	chr3	147402104	624	+	RI	ZIC4	1.53	0.012*	1.16, 2.35
chr4_157677227_NE	chr4	157677227	107	+	NE	LOC105377509	1.34	0.050*	1.01, 1.90

B

Loci	chr	start	size	strand	SV type	genes	OR	p-value	95% CI
chr8_69118424_NE	chr8	69118424	86	-	NE	LINC01592	1.29	0.148	0.97, 3.75
chr4_157677227_NE	chr4	157677227	107	+	NE	LOC105377509	1.34	0.050*	1.01, 1.90

C

SV	chr	start	size	strand	SV type	genes	OR	p-value	95% CI
chr20_63241753_RI	chr20	63241753	709	+	RI	NKAIN4	1.38	0.151	0.94, 2.39
chr3_147402104_RI	chr3	147402104	624	+	RI	ZIC4	1.54	0.011*	1.17, 2.36

D

SV	chr	start	size	strand	SV type	genes	OR	p-value	95% CI
chr11_2149345_PNJ	chr11	2149345	127	+	PNJ	IGF2|IGF2-AS|INS-IGF2	1.96	0.047*	1.20, 5.39
chr12_21334709_PNJ	chr12	21334709	365	+	PNJ	SLCO1A2	2.43	0.302	0.78, 85.11
chr8_139601601_PNJ	chr8	139601601	457	+	PNJ	KCNK9	1.67	0.106	1.03, 4.11

E

SV	chr	start	size	strand	SV type	genes	OR	p-value	95% CI
chr12_57216843_UN	chr12	57216843	40	-	UN	NXPH4	1.38	0.212	0.95, 3.13
chr14_105863814_UN	chr14	105863814	36	+	UN	ADAM6|LINC00221	1.52	0.045*	1.08, 2.62

Supplementary Figure S11. Multivariate analysis of all SV for cases vs controls. **A.** Multivariate analysis with all 6,003 selected SV in multiple univariate analyses. **B.** Multivariate analysis with only novel exon (NE) selected SV in univariate analyses. **C.** Multivariate analysis with only retained intron (RI) selected SV in univariate analyses. **D.** Multivariate analysis with only partial novel junction (PNJ) selected SV in univariate analyses. E. Multivariate analysis with only unknown (UN) selected SV in univariate analyses.

SV: structural variant. NE: novel exon -- an aligned block that does not cross any existing exons. May be intronic or intergenic. RI: retained intron -- a contig block that spans a whole intron. PNJ: partial novel junction -- spliced contig where one junction matches a known boundary (the other side is unknown). UN: unknown -- by default, all soft-clipped contigs are classified as unknown at the moment. * Significant at a p-value < 0.05.

A

SV	OR
chr10_101729717_NE	1.95
chr11_2149345_PNJ	1.52
chr11_89498187_AS	1.54
chr13_55179004_NE	1.11
chr14_105743009_NE	1.17
chr14_105863198_NE	1.08
chr14_105863814_UN	1.14
chr14_105986593_FUS	1.11
chr19_8876368_IGR	1.31
chr20_33053965_NEJ	1.63
chr21_8259383_NE	1.52
chr3_147402104_RI	1.35
chr5_102458491_AS	1.29
chr5_102608496_INS	1.22
chr5_148089622_EE	1.16
chr5_85663902_NEJ	1.77
chr6_170156045_AS	1.32

B

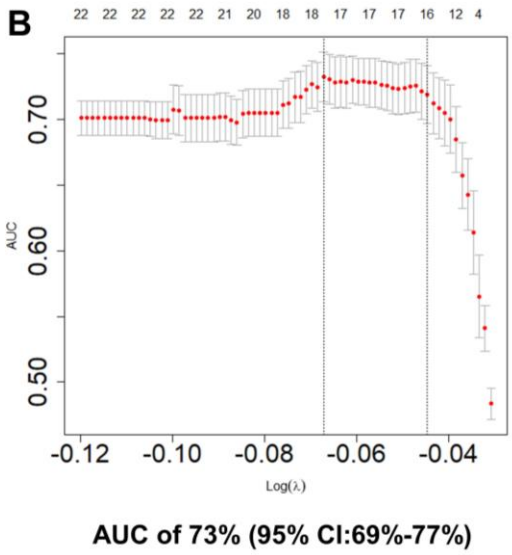

Supplementary Figure S12. Multivariate Lasso prediction model of HGSC with SVs. 22 SV were initially selected in ANOVA univariate analyses with cross-validation out of the total 32,156 SVs. **A.** The lasso multivariate prediction analysis identified 17 SV that predicted HGSC with an AUC of 73%. **B.** Prediction model with performance by AUC of 0.73 (95% CI: 69%-77%).

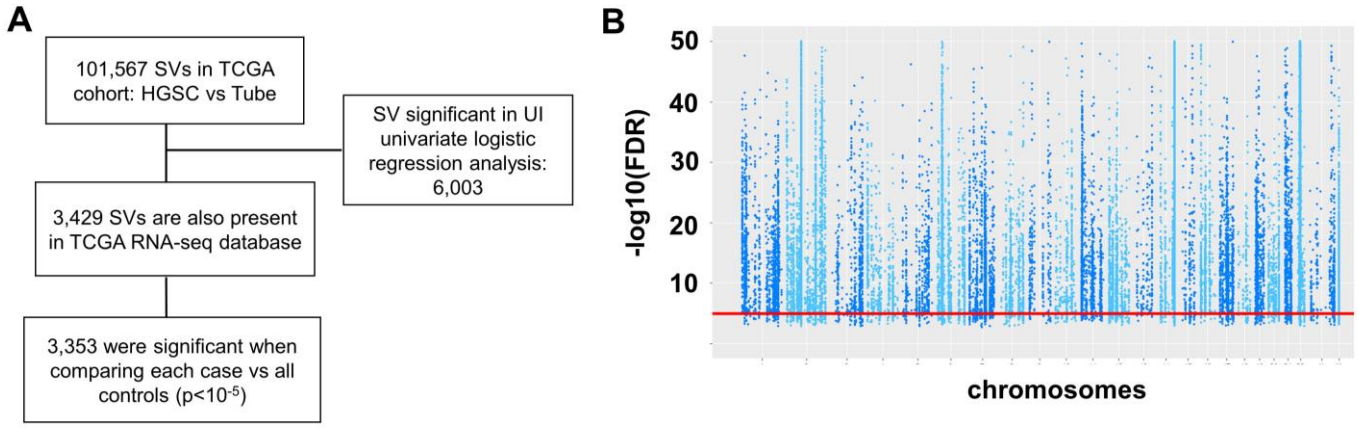

C

SV	chr	start	size	strand	SV type	genes	OR	p-value	95% CI
chr11_2149345_PNJ	chr11	2149345	127	+	PNJ	IGF2|IGF2-AS|INS-IGF2	3.08	0.056	1.58, 34.63
chr14_105863814_UN	chr14	105863814	36	+	UN	ADAM6|LINC00221	1.14	0.068	1.002, 1.35

Supplementary Figure S13. Validation of structural variation (SV) between HGSC samples and tubal controls in TCGA dataset. Analysis performed with MINTIE. Controls were taken from same tubal RNA-seq experiments used for the UI dataset. **A.** All SV for each individual case (371), each one compared to controls (12). 3,429 SVs out of 6,003 selected in the UI analysis, were also present in TCGA dataset. 3,353 of those were significant when compared with controls in the MINTIE analysis, with a FDR <0.05 and log2 fold change >2. **B**. Selected SV are represented in a Manhattan plot. **C.** Multivariate analysis with all SV significant in the UI multivariate analysis: 2 SV were independently significant.

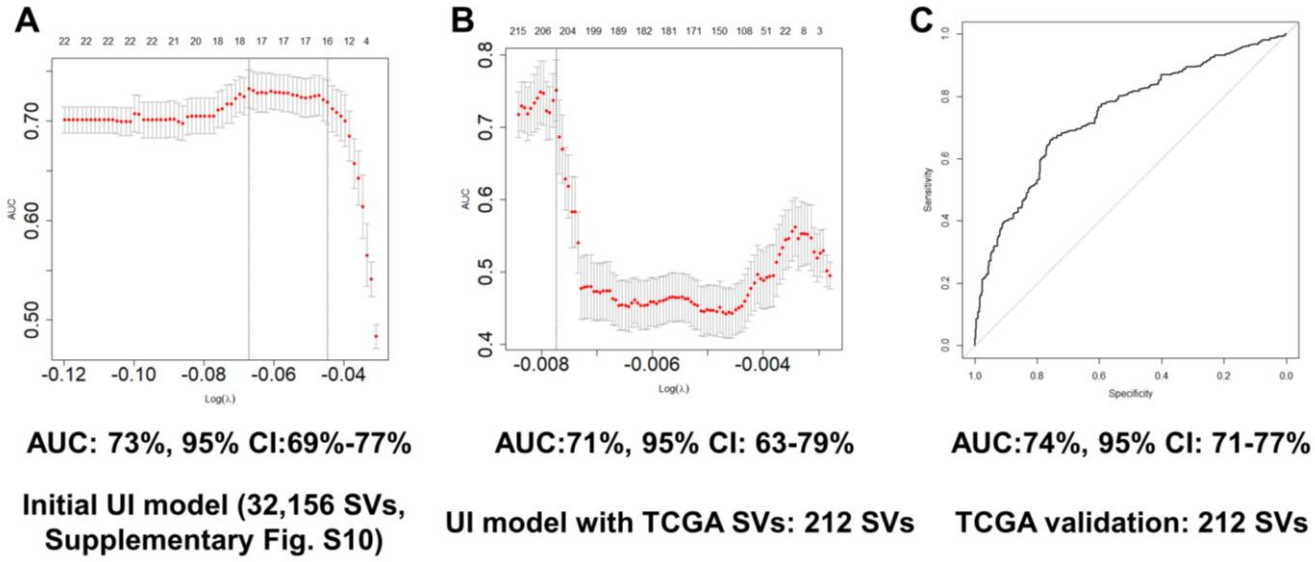

Supplementary Figure S14. Validation of multivariate lasso prediction analysis of structural variation (SV). **A.** Original lasso prediction model of HGSC with final 17 SV included in the model. **B.** UI lasso prediction model of the 3,429 SVs (out of 6,003) that were selected and present in TCGA database. The prediction model was comprised of 212 SVs for an AUC of 71%. **C.** Validation of the UI multivariate analysis in TCGA dataset, with a good performance of an AUC of 74%, accuracy of 63%, sensitivity of 85%, and PPV of 73%.